Volumetric Behavior of Nitrous Oxide

Pressure-Volume Isotherms at High Pressures

EARL J. COUCH[1] and KENNETH A. KOBE[2]

Gas Compressibility Factors at Low Pressures

LEO J. HIRTH[3] and KENNETH A. KOBE[2]
University of Texas, Austin 12, Tex.

NITROUS OXIDE is used extensively as a low temperature refrigerant. In such applications, a knowledge of its physical and thermodynamic properties is especially desirable.

Although the *P-V-T* properties of nitrous oxide have been studied for over a hundred years, the data reported by previous investigators are limited primarily to the saturation region and, in many cases, are not in agreement. For example, vapor pressure measurements (*4, 10, 19, 24, 32*) show differences as great as 20%. Similar deviations are found in the orthobaric densities reported for nitrous oxide (*5, 10, 12, 14, 20, 24, 27, 33*). Previous gas compressibility data, other than the measurements at low pressures (*3, 8, 22*), are limited to the temperature range 20° to 67° C. (*4, 7, 21*). The more recent compressibility measurements of Hirth (*18*) cover the range from −30° to 150° C. for pressures up to 65 atm. Reliable *P-T-V* data for liquid nitrous oxide have not been reported in the literature.

In this article, experimental pressure-volume isotherms from −30° to 150° C. for the pressure range 6 to 315 atm. are presented, as well as derived quantities, including smoothed vapor pressures, the critical constants, orthobaric densities, and calculated latent heats of vaporization.

EXPERIMENTAL

Nitrous Oxide Purity. A cylinder of pharmaceutical grade nitrous oxide obtained from the Stuart Oxygen Co. was 99.7% pure, with nitrogen as the principal impurity. This gas was further purified by vacuum distillation at liquid nitrogen temperature. On the basis of change in vapor pressure upon isothermal condensation, the purity of the nitrous oxide used in this work was estimated to be 99.998%.

Equipment and Method. The apparatus is of the same basic design as that described by Keyes (*23*) and Beattie (*2*).

Construction, calibration, and operation of the equipment have been described (*11, 15*). Briefly, temperatures were measured to ±0.002° C. and controlled within ±0.003° C. by means of a calibrated platinum resistance thermometer used in conjunction with a Type G-1 Müller bridge and a photoelectric relay circuit actuated by a sensitive optical galvanometer. Pressures were measured with a dead weight gage calibrated against the vapor pressure of carbon dioxide.

Volume was measured by means of a calibrated mercury injector pump with an estimated accuracy of ±0.005 ml. The mass of the gas sample, introduced into the *P-V-T* cell by the usual weighing bomb techniques (*2, 9*), was established within ±0.2 mg.

Results. The experimental *P-V-T* measurements on nitrous oxide include the gas phase compressibility factors (Figure 1), liquid phase volumes (Figure 2), pressure-volume isotherms near the critical point (Figure 3), and vapor pressure data (Figure 4). In obtaining these results, measurements were made on three samples of nitrous oxide:

Sample No.	Mass, Grams	Specific Vol. Range, Ml./G.
1	0.5139	4.5 to 84
2	2.0362	0.9 to 21
3	6.0290	0.9 to 7

The agreement of the data in the overlapping volume ranges covered by these samples indicates a reproducibility of ±0.002 ml. per gram in the measured specific volumes.

The estimated maximum error in the experimentally measured quantities is:

Temperature, ° C.	±0.02	Sample mass, %	±0.04
Pressure, %	±0.04	Volume, %	±0.1

[1] Present address, Field Research Laboratory, Socony Mobil Oil Co., Dallas, Tex.
[2] Deceased.
[3] Present address, Esso Research & Engineering Co., Florham Park, N. J.

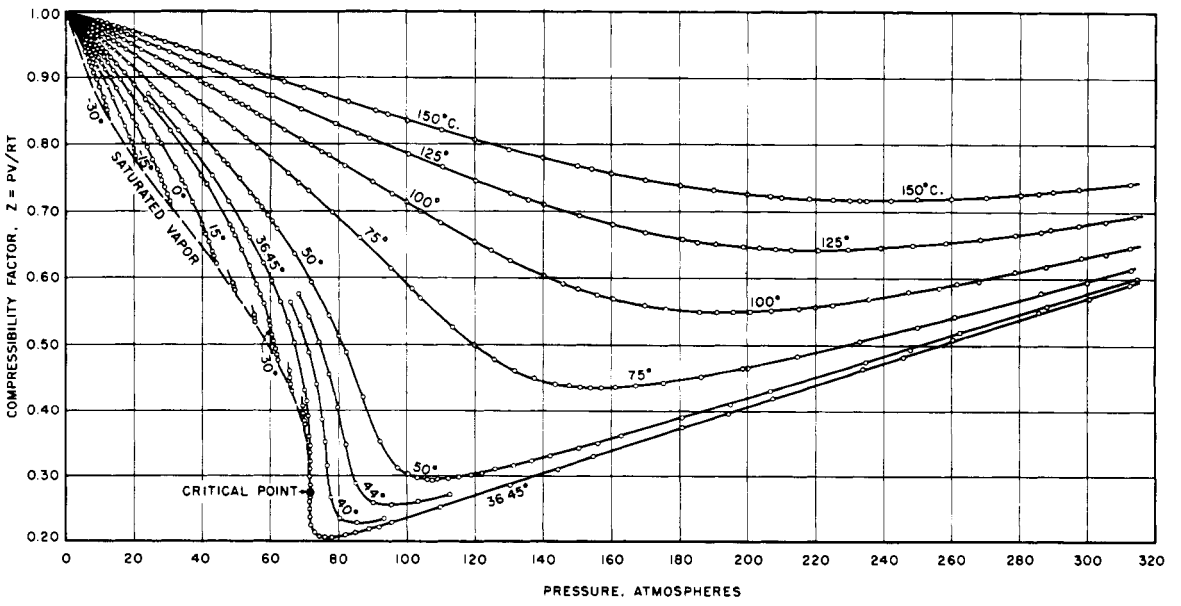

Figure 1. Compressibility factors of nitrous oxide

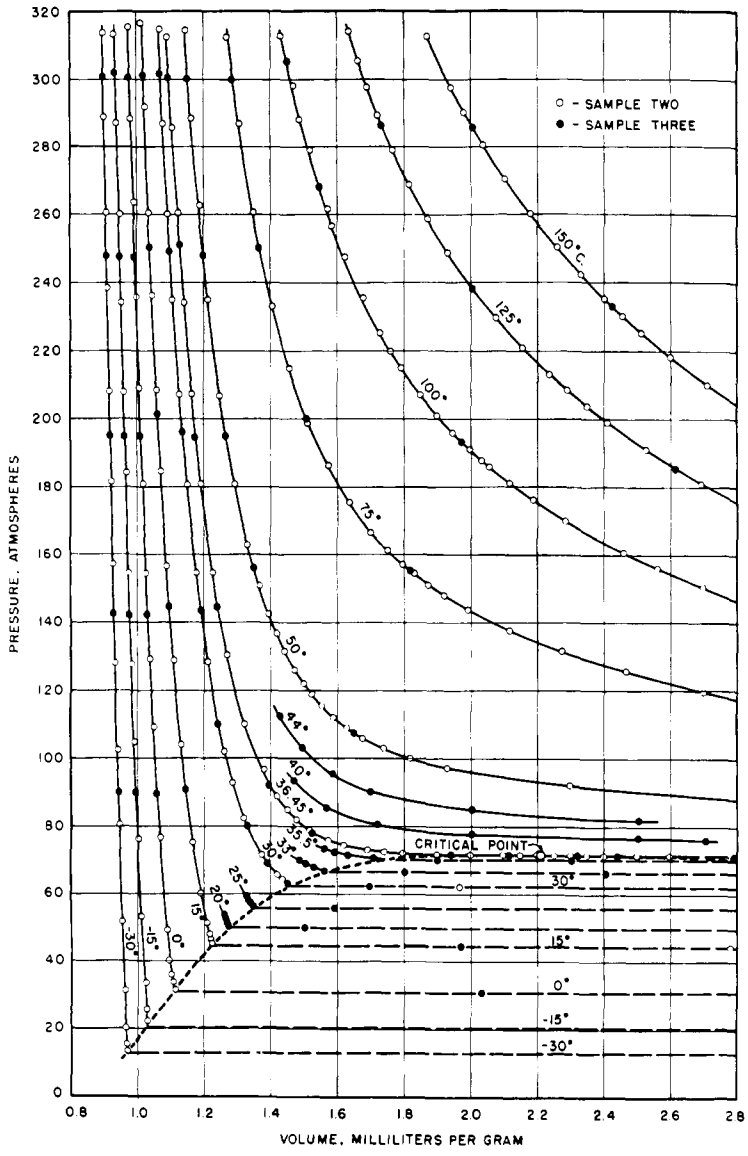

Figure 2. Pressure-volume isotherms of liquid nitrous oxide

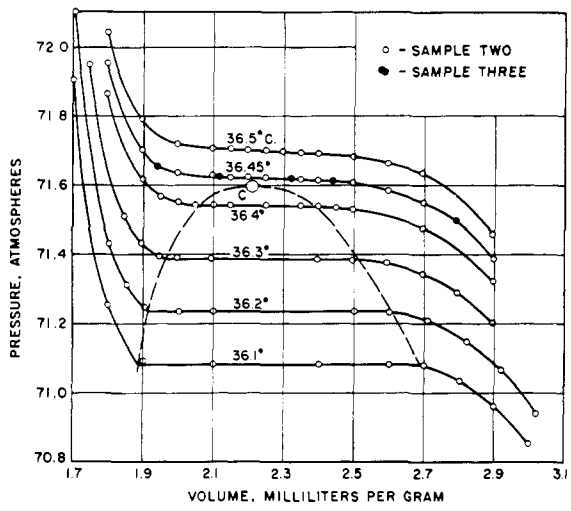

Figure 3. Isotherms near the critical point of nitrous oxide

Table I. Smoothed Pressure-Volume Isotherms of Liquid Nitrous Oxide

Pressure, Atm.	Temperature, ° C. −30	−15	0	15	30
	Specific Volume, Ml./G.				
315	0.8976	0.9347	0.9738	1.0160	1.0644
300	0.8998	0.9377	0.9775	1.0206	1.0711
280	0.9030	0.9420	0.9827	1.0274	1.0808
260	0.9064	0.9465	0.9881	1.0346	1.0914
240	0.9099	0.9511	0.9939	1.0424	1.1031
220	0.9134	0.9558	1.0002	1.0513	1.1160
200	0.9171	0.9609	1.0069	1.0615	1.1307
180	0.9210	0.9663	1.0141	1.0726	1.1480
160	0.9252	0.9720	1.0221	1.0849	1.1685
140	0.9296	0.9780	1.0309	1.0987	1.1929
120	0.9342	0.9844	1.0406	1.1145	1.2234
100	0.9390	0.9912	1.0513	1.1333	1.2632
90	0.9414	0.9949	1.0571	1.1443	1.2912
80	0.9439	0.9987	1.0631	1.1565	1.3271
70	0.9464	1.0027	1.0694	1.1702	1.3827
60	0.9491	1.0070	1.0763	1.1868	...
50	0.9519	1.0115	1.0839	1.2077	...
40	0.9551	1.0163	1.0929	...	...
30	0.9587	1.0216	...	...	...
20	0.9630	...	...	...	...

The corresponding maximum error in the calculated compressibility factors is 0.2%.

The uncertainty in the vapor pressure measurements is somewhat higher, primarily because of difficulty in determining when thermal equilibrium was attained during the course of traversing the two-phase region. Measurements for the various samples show differences as great as 0.06 atm. at the lower temperatures. The average difference of 0.03 atm. corresponds to an average error of 0.2% in the vapor pressure data.

The experimental data shown in Figures 1 through 4 have been tabulated (*11*).

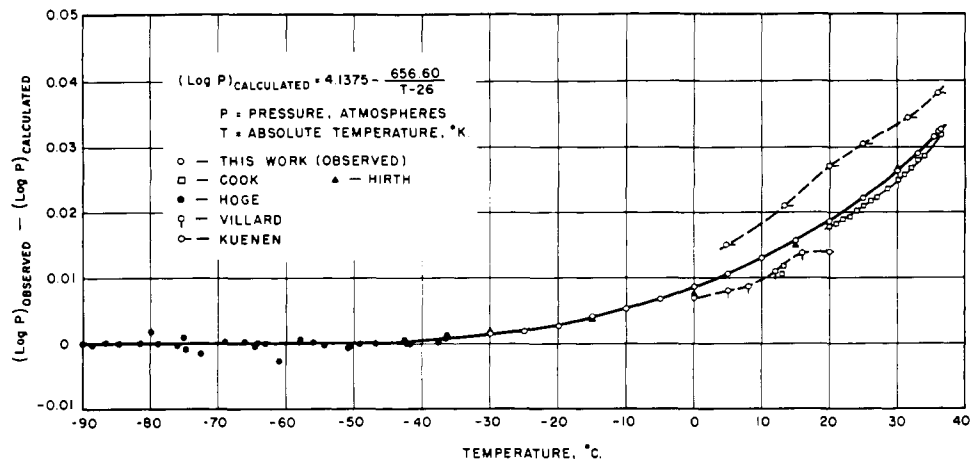

Figure 4. Vapor pressure data for nitrous oxide

DERIVED QUANTITIES

Smoothed *P-V-T* Values. In smoothing the experimental liquid data shown in Figure 2, the method of graphical residuals was employed. Each isotherm was approximated by a straight line of the form $v = a + bP$, the constants being evaluated from two arbitrarily selected experimental points at the extremes of the pressure range. The residuals of the experimental data from the approximating line were smoothed graphically and the smoothed residuals then employed in calculating the values of Table I.

Smoothed compressibility data for the gas phase are presented in Table II. For pressures below 60 atm., these values were obtained from a large scale plot of compressibility factor, $z = PV/RT$, *vs.* pressure. At higher pressures, residual volume isotherms calculated from Equation 1

$$\alpha = RT/P - V \quad (1)$$

were smoothed graphically with respect to pressure. These smoothed residual volumes were then used in conjunction with Equation 1 in evaluating the specific volumes and compressibility factors of Table II. No systematic differences were incurred in this smoothing process.

Hirth (*18*), in comparing his measurements with the compressibility factors of Table II at selected pressures up

Table II. Smoothed Compressibility Data for Gaseous Nitrous Oxide

Pressure, Atm.	Vol., Ml./G.	$z = PV/RT$	Pressure, Atm.	Vol., Ml./G.	$z = PV/RT$	Pressure, Atm.	Vol., Ml./G.	$z = PV/RT$	Pressure, Atm.	Vol., Ml./G.	$z = PV/RT$
	−30° C.			15° C.			36.45° C.			40° C.	
6	70.533	0.9336	6	86.201	0.9628	25	20.074	0.8695	68	4.610	0.5370
7	59.686	0.9217	8	63.811	0.9503	30	16.144	0.8391	70	4.234	0.5077
8	51.540	0.9096	10	50.351	0.9373	35	13.313	0.8073	72	3.838	0.4733
9	45.179	0.8970	12	41.350	0.9237	40	11.158	0.7733	74	3.377	0.4281
10	40.058	0.8837	15	32.331	0.9028	45	9.450	0.7368	76	2.758	0.3591
11	35.848	0.8699	20	23.266	0.8662	50	8.045	0.6969	78	1.955	0.2612
12	32.301	0.8551	25	17.774	0.8272	55	6.843	0.6521	80	1.737	0.2380
	−15° C.		30	14.035	0.7838	60	5.776	0.6004	85	1.576	0.2294
			35	11.281	0.7350	65	4.752	0.5352	90	1.506	0.2321
6	75.903	0.9463	40	9.131	0.6799	68	4.098	0.4828			
8	55.796	0.9275	42	8.362	0.6538	70	3.555	0.4312		44° C.	
10	43.674	0.9075	44	7.628	0.6248	71	3.173	0.3903			
12	35.557	0.8866		30° C.		72	1.792	0.2235	68	5.039	0.5795
14	29.725	0.8647				74	1.636	0.2097	70	4.715	0.5582
15	27.377	0.8533	6	91.243	0.9687	76	1.567	0.2063	72	4.386	0.5341
16	25.317	0.8417	8	67.691	0.9582	78	1.527	0.2063	74	4.059	0.5080
18	21.876	0.8182	10	53.537	0.9473	80	1.498	0.2076	76	3.722	0.4784
20	19.019	0.7904	12	44.096	0.9363	90	1.409	0.2197	78	3.360	0.4432
	0° C.		15	34.629	0.9191	100	1.3547	0.2347	80	2.969	0.4017
			20	25.132	0.8894	120	1.2913	0.2685	82	2.526	0.3503
6	81.102	0.9556	25	19.403	0.8583	140	1.2490	0.3030	85	2.000	0.2875
8	59.840	0.9401	30	15.532	0.8245	160	1.2160	0.3371	90	1.705	0.2595
10	47.062	0.9242	35	12.738	0.7889	180	1.1906	0.3713	95	1.592	0.2558
12	38.510	0.9075	40	10.614	0.7512	200	1.1695	0.4052	100	1.526	0.2581
15	29.922	0.8814	45	8.895	0.7083	220	1.1512	0.4388	105	1.479	0.2627
20	21.268	0.8353	50	7.467	0.6606	240	1.1354	0.4721	110	1.443	0.2685
25	15.959	0.7835	55	6.204	0.6038	260	1.1215	0.5052			
28	13.633	0.7496	58	5.470	0.5614	280	1.1086	0.5378			
29	12.934	0.7366	60	4.964	0.5270	300	1.0967	0.5700			
30	12.266	0.7226	62	4.391	0.4817	315	1.0886	0.5941			

	50° C.		75° C.			100° C.		125° C.		150° C.	
Pressure, Atm.	Vol., ml./g.	$z = PV/RT$	Vol., ml./g.	$z = PV/RT$	Pressure, Atm.	Vol., ml./g.	$z = PV/RT$	Vol., ml./g.	$z = PV/RT$	Vol., ml./g.	$z = PV/RT$
8	72.797	0.9667	79.053	0.9744	8	85.225	0.9801	91.343	0.9845	97.423	0.9880
10	57.719	0.9581	62.808	0.9677	10	67.818	0.9749	72.785	0.9806	77.694	0.9849
15	37.580	0.9357	41.140	0.9508	15	44.609	0.9619	48.018	0.9704	51.381	0.9770
20	27.498	0.9129	30.287	0.9333	20	32.998	0.9487	35.617	0.9597	38.196	0.9684
30	17.344	0.8637	19.408	0.8971	30	21.352	0.9208	23.215	0.9383	25.020	0.9515
40	12.208	0.8106	13.945	0.8594	40	15.522	0.8925	17.001	0.9162	18.424	0.9342
50	9.070	0.7528	10.644	0.8200	50	12.012	0.8634	13.273	0.8941	14.468	0.9170
60	6.905	0.6877	8.421	0.7785	60	9.668	0.8339	10.789	0.8721	11.834	0.9001
70	5.254	0.6105	6.815	0.7350	70	7.990	0.8040	9.017	0.8503	9.955	0.8834
80	3.862	0.5129	5.592	0.6893	80	6.728	0.7737	7.688	0.8286	8.551	0.8672
90	2.559	0.3823	4.622	0.6409	90	5.745	0.7433	6.656	0.8071	7.460	0.8511
100	1.824	0.3028	3.835	0.5909	100	4.961	0.7131	5.833	0.7858	6.591	0.8355
110	1.613	0.2945	3.197	0.5419	110	4.321	0.6833	5.163	0.7651	5.883	0.8204
120	1.513	0.3014	2.692	0.4977	120	3.793	0.6543	4.611	0.7454	5.297	0.8058
130	1.449	0.3127	2.320	0.4648	130	3.359	0.6278	4.149	0.7266	4.805	0.7919
140	1.404	0.3263	2.064	0.4452	140	3.002	0.6041	3.760	0.7092	4.390	0.7791
150	1.368	0.3407	1.886	0.4359	150	2.709	0.5841	3.430	0.6932	4.033	0.7669
160	1.339	0.3557	1.763	0.4346	160	2.472	0.5685	3.152	0.6795	3.729	0.7563
170	1.315	0.3710	1.674	0.4384	170	2.281	0.5574	2.914	0.6675	3.465	0.7468
180	1.293	0.3863	1.607	0.4456	180	2.129	0.5508	2.714	0.6581	3.235	0.7381
190	1.274	0.4018	1.552	0.4543	190	2.008	0.5484	2.543	0.6509	3.035	0.7310
200	1.258	0.4176	1.508	0.4647	200	1.908	0.5486	2.396	0.6457	2.861	0.7254
220	1.230	0.4492	1.440	0.4882	220	1.757	0.5557	2.164	0.6414	2.576	0.7183
240	1.207	0.4808	1.388	0.5132	240	1.652	0.5698	1.992	0.6440	2.353	0.7159
260	1.188	0.5106	1.349	0.5404	260	1.573	0.5878	1.862	0.6522	2.178	0.7179
280	1.170	0.5438	1.317	0.5682	280	1.510	0.6080	1.761	0.6643	2.038	0.7235
300	1.154	0.5746	1.287	0.5949	300	1.462	0.6304	1.681	0.6795	1.928	0.7334
315	1.145	0.5987	1.266	0.6144	315	1.428	0.6468	1.632	0.6928	1.860	0.7429

to 60 atm., found agreement generally within 0.2%. The maximum difference of 0.5% occurring at 30° C. and 62 atm., is well within the estimated error for the two experimental methods.

The isotherms near the critical point presented in Table III were obtained by graphically smoothing the experimental data shown in Figure 3.

Vapor Pressures. The observed pressure at each temperature in Table IV represents the average of the vapor pressure measurements performed on the three samples of nitrous oxide at various specific volumes in the two-phase region. These observed pressures were smoothed by the method of graphical residuals. Based on the equation of Hoge (*19*),

$$\text{Log } P = A - 1/T\,[B + Cy(10^{Dy^2} - 1)] + r_p \qquad (2)$$

where

$$y = 69{,}500 - T^2$$
$$A = 4.52620$$
$$C = 1.157 \times 10^{-4}$$
$$B = 829.148$$
$$D = 3.4 \times 10^{-10}$$

Table III. Smoothed Isotherms in Critical Region of Nitrous Oxide

Specific Vol., Ml./G.	Temperature, ° C. 36.1	36.2	36.3	36.4	36.45	36.5
	Pressure, Atm.					
3.00	70.854	70.971	...	...	...	...
2.90	70.961	71.084	71.197	71.317	71.380	71.448
2.80	71.034	71.161	71.286	...	71.491	...
2.70	71.078	71.212	71.340	71.473	71.545	71.633
2.60	71.082	71.236	71.374	...	71.581	71.661
2.50	...	71.236	71.389	71.528	71.606	71.680
2.45	...	...	...	71.536	71.612	...
2.40	71.082	...	71.389	71.541	71.615	71.691
2.35	...	...	...	71.543	71.617	71.694
2.30	...	...	...	...	71.619	71.697
2.25	...	...	...	71.543	71.620	71.699
2.20	...	...	...	...	71.621	71.700
2.15	...	...	...	71.543	71.622	71.702
2.10	71.082	71.236	71.389	71.543	71.623	71.705
2.05	...	...	...	71.544	...	...
2.00	...	71.236	71.389	71.550	71.634	71.718
1.95	...	...	71.393	71.566	71.649	...
1.90	71.082	71.251	71.427	71.615	71.697	71.788
1.85	...	71.320	71.502	...	...	...
1.80	71.258	71.446	...	71.860	71.947	72.040
1.75	...	...	71.935	...	...	...
1.70	71.940	72.142	...	...	...	...

the residual, r_p, was calculated for each observed vapor pressure. These residuals were smoothed graphically and used in conjunction with Equation 2 in evaluating the smoothed vapor pressures of Table IV.

Figure 4 compares the vapor pressure data of the present work with the values reported by Cook (*10*), Hirth (*18*), Hoge (*19*), Keunen (*24*), and Villard (*32*). The ordinate of this plot is the difference between the logarithm of the observed vapor pressure, log $P_{obsd.}$, and that calculated from

$$\text{Log } P_{calcd.} = 4.1375 - \frac{626.60}{T - 26} \qquad (3)$$

This relation (Antoine equation), derived by Hoge (*19*) in representing his low temperature measurements, shows the characteristic deviations at higher temperatures but serves as a convenient datum for comparing the several sets of data. The vapor pressure data reported by Cook (*10*) and Hirth (*18*) are in particularly good agreement with those of the present work.

Orthobaric Densities. The observed orthobaric densities (Table IV) were obtained by extrapolating the experimental pressure-volume isotherms to the corresponding smoothed vapor pressure and were fitted to the Equations 4 and 5 by the least squares method.

$$(d_L + d_g)/2 = 0.495800 - 0.00124027\,t + r_d \qquad (4)$$

$$(d_L - d_g)/2 = 0.12595\,(t_c - t)^{1/3} - 0.008966 + r_e \qquad (5)$$

where $t_c = 36.434°$ C.

The residuals r_d and r_e, defined by Equations 4 and 5, respectively, were smoothed graphically with respect to temperature. These smoothed residuals were then used with Equations 4 and 5 in evaluating the smoothed orthobaric densities of Table IV.

In Figure 5, the smoothed orthobaric densities are shown in comparison with those reported by other investigators. The curve through the values here reported passes well within the scatter of the literature data and joins smoothly with the low temperature data (*20*). The orthobaric densities of the present work are in good agreement with those reported by Cook (*10*), Hirth (*18*), and Villard (*33*).

Critical Point. The critical temperature, corresponding to that isotherm having a horizontal point of inflection on a pressure *vs.* volume plot, was determined by visual inspection of Figure 3 to be approximately 36.45° C. This value was adjusted to obtain the characteristic behavior of

Table IV. Properties of Saturated Nitrous Oxide

Temp., ° C.	Vapor Pressure, Atm. Observed	Smoothed	Orthobaric Densities, G./Ml. Observed Vapor	Observed Liquid	Smoothed Vapor	Smoothed Liquid	Latent Heat of Vaporization, Cal./G. Observed	Smoothed
−30	13.044	13.041	0.03430	1.0341	0.03429	1.0344	69.817	69.788
−25	15.267	15.274	...	...	0.04040	1.0149	67.590	67.575
−20	17.772	17.778	...	...	0.04732	0.9947	65.280	65.318
−15	20.582	20.571	0.05462	0.9735	0.05509	0.9738	63.007	62.995
−10	23.665	23.670	...	...	0.06397	0.9516	60.575	60.573
−5	27.090	27.096	...	...	0.07409	0.9285	58.013	58.014
0	30.878	30.869	0.08541	0.9039	0.08569	0.9039	55.274	55.272
5	35.007	35.013	...	...	0.09920	0.8777	52.247	52.249
10	39.546	39.552	...	...	0.11515	0.8491	48.853	48.861
15	44.511	44.514	0.13436	0.8173	0.13436	0.8176	45.001	44.997
20	49.937	49.934	0.15895	0.7841	0.15827	0.7817	40.494	40.499
25	55.856	55.850	0.18987	0.7401	0.18939	0.7389	35.056	35.054
30	62.322	62.318	0.23381	0.6824	0.23382	0.6830	27.956	27.960
33	66.484	66.497	0.27451	0.6352	0.27440	0.6359	22.018	22.017
35.5	70.154	70.173	0.3375	0.5674	0.3381	0.5676	13.481	13.485
36.1	71.082	71.082	0.3711	0.5302	0.3728	0.5320	9.180	9.152
36.2	71.235	71.236	0.3836	0.5230	0.3828	0.5220	7.989	7.974
36.3	71.386	71.389	0.3978	0.5097	0.3965	0.5083	6.379	6.379
36.4	71.540	71.543	0.4188	0.4854	0.4191	0.4857	3.776	3.776
36.434	...	71.596	...	...	0.4525	0.4525	0.000	0.000

the saturation curve near the critical point (*29*). By successive trials, the value of t_c for which $(d_l - d_g)$ showed the proper dependence on $(t_c - t)^{1/3}$ was determined to be 36.434° C. With this value of the critical temperature, the critical pressure was calculated from Equation 2 and the critical density was calculated from the rectilinear diameter given by Equation 4. The resulting critical properties of nitrous oxide are:

$$t_c = 36.434° \pm 0.005° \text{ C.}$$
$$P_c = 71.596 \pm 0.007 \text{ atm.}$$
$$d_c = 0.4525 \pm 0.001 \text{ gram per ml.}$$

These values are shown in comparison with the critical constants reported by other investigators in Table V.

Latent Heat of Vaporization. The observed latent heat values presented in Table IV were evaluated by use of the Clapeyron equation,

$$\Delta H_v = JT(v_g - v_L)(dP/dT) \quad (6)$$

in conjunction with the smoothed orthobaric densities of Table IV and the vapor pressure relation given by Equation 2. In evaluating the slope of the vapor pressure curve, the residual term, r_p, was differentiated and smoothed graphically. This residual derivative, dr_p/dT, contributed a maximum of 1% to the slope of the vapor pressure curve calculated from Equation 2.

In smoothing the latent heat data, the observed values were fitted to the equation:

$$\Delta H_v = a(t_c - t)^b + c(t_c - t) + r_v \quad (7)$$

Table V. Comparison of Critical Properties

Date	t_c, ° C.	P_c, Atm.	d_c, G./Ml.	Investigator
1956	36.434	71.596	0.4525	This work
1953	36.39	71.4	0.452	Cook (*10*)
1929	...	...	0.459	Quinn and Wernimont (*27*)
1912	36.50	71.65	...	Cardoso and Arni (*6*)
1895	36.0	71.9	...	Kuenen (*24*)
1894	38.8	77.5	0.454	Villard (*33*)
1886	...	...	0.41	Cailletet and Mathias (*5*)
1884	35.4	75.0	...	Dewar (*13*)
1878	36.4	73.07	...	Janssen (*21*)

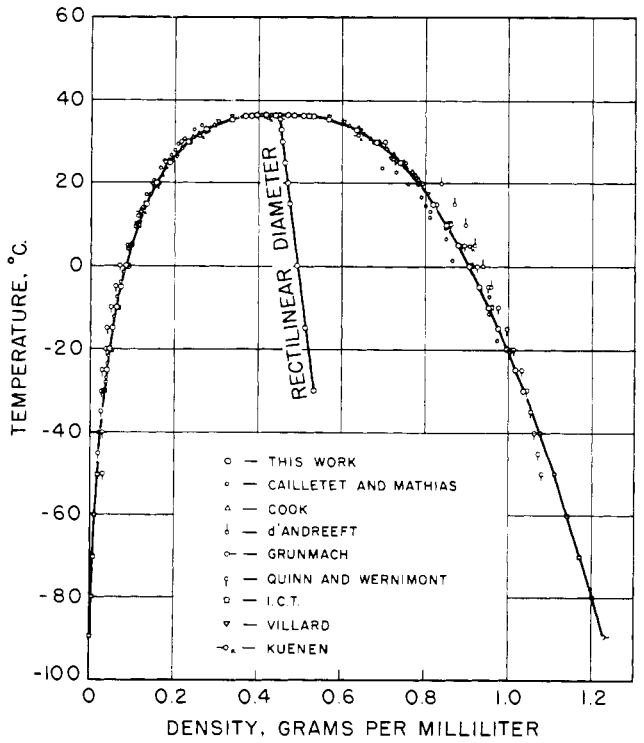

Figure 5. Orthobaric densities of nitrous oxide

where

$$a = 12.9922$$
$$c = -0.082167$$
$$b = 0.417796$$
$$t_c = 36.434° \text{ C.}$$

The residuals, r_v, were smoothed graphically and the smoothed latent heats calculated from Equation 7 are shown in Table IV. These latent heat data are considered to be reliable to 1% for temperatures below 35° C.

CONCLUSIONS

While the accuracy of the experimental *P-V-T* measurements is discussed above, a realistic estimation of the reliability of the derived quantities is difficult. In some cases, notably the orthobaric densities and latent heat values, the above tabulations contain more significant figures than the probable accuracy warrants. These additional figures have been retained not only as an indication of the internal consistency of the smoothed tabulations, but also with a view to the possible use of these data in subsequent thermodynamic calculations wherein differences and differential coefficients must be evaluated. In using the data as such, the limitations on their reliability should be borne in mind.

Gas Compressibility Factors at Low Pressures

The pressure range of the gas compressibility factor isotherms is extended to pressures as low as 1 atm. over the temperature range −30° to 150° C. Also given are smoothed values of the second virial coefficient for nitrous oxide, parameters for use with the Lennard-Jones potential function which predicts values of the second virial coefficient, and fugacity coefficients for gaseous nitrous oxide for pressures up to 315 atm. over the temperature range from −30° to 150° C.

EXPERIMENTAL

Nitrous Oxide Purity. The nitrous oxide used is described above. It was further purified by cooling to −70° C. and then discharging gas from the vapor phase until the original weight was reduced by 10%.

Apparatus. The design, construction, and calibration of the Burnett apparatus used in this investigation are described by Silberberg, Kobe, and McKetta (*30*). The equipment was modified to extend the lower temperature limit to −30° C.

RESULTS

Compressibility. The compressibility factor is defined as

$$z = PV/RT \quad (8)$$

The experimental data were treated graphically (*30*). Large scale plots of $P_r N^r$ *vs.* P_r were made to determine P_o/z_o, the ordinate at zero pressure. On these plots ordinates could be read to 0.01 to 0.02% with commensurate precision for the abscissas. The compressibility factor, z_r, at each pressure, P_r, was calculated by dividing each $P_r N^r$ by P_o/z_o.

Compressibility factor isotherms were measured at 15° C. intervals from −30° to 30° C. for pressures ranging from atmospheric to slightly below the vapor pressure. Between 50° and 150° C. the isotherm increment was 25° C. and pressures up to 65 atm. were measured. However, since the gas compressibility factors at the higher pressures agree so well with Couch's results (*11*), only the experimental data below 10 atm. are shown in Table VI.

The maximum error, including that from pressure and temperature, in the compressibility factor values of Table